

PAPER • OPEN ACCESS

## The acoustic response of stiffened plates

To cite this article: D Zhao *et al* 2019 *J. Phys.: Conf. Ser.* **1264** 012041

View the [article online](#) for updates and enhancements.

### You may also like

- [A comparative experimental study on sample excitation and probe excitation in force modulation atomic force microscopy](#)  
Chunlai Yang, Yuhang Chen, Tian Wang et al.
- [Loss of gas from echogenic liposomes exposed to pulsed ultrasound](#)  
Jason L Raymond, Ying Luan, Tao Peng et al.
- [Non-contact test set-up for aeroelasticity in a rotating turbomachine combining a novel acoustic excitation system with tip-timing](#)  
O Freund, M Montgomery, M Mittelbach et al.



The Electrochemical Society  
Advancing solid state & electrochemical science & technology

243rd ECS Meeting with SOFC-XVIII

Boston, MA • May 28 – June 2, 2023

**Abstract Submission Extended  
Deadline: December 16**

[Learn more and submit!](#)

# The acoustic response of stiffened plates

**D Zhao, G Squicciarini and N S Ferguson**

Institute of Sound and Vibration Research, University of Southampton, Southampton  
SO17 1BJ, UK

Dong.Zhao@soton.ac.uk

**Abstract.** For acoustic fatigue and other applications, including sound transmission through panels, one feature is the means in which acoustic excitation produces the subsequent structural response. This study revisits the acoustic excitation of stiffened flat homogeneous plates using an approximate model for evaluating the modal characteristics. Excitation of the modes are considered and compared to the formulation of the Joint Acceptance for plane wave harmonic acoustic excitation. The latter being typically used for single panels or more general aerospace structural configurations. Numerical simulations are then given. These illustrate the effect of the stiffeners on the resulting displacement and stress response, in comparison to both stiffened and separately orthogonally stiffened plate arrangements. In addition, the paper interprets and highlights the effect of the surface area, angle of incidence and contribution of different mode to the behaviour.

## 1. Introduction

The actual practical application of the acoustic response prediction for structures came to the forefront of aeronautical interest with the introduction of high capacity gas turbine engines. The resulting jet noise potentially impinging onto the structure of supersonic aircraft or launch vehicles give rise to problematic vibrations throughout the flight [1]. As the interest was primarily focused on the durability and fatigue of aircraft, much attention was on the linear dynamics of the fuselage and latterly wing structures comprising stiffened skins. Flat plates reinforced by orthogonal beams are used extensively in aerospace vehicles, where acoustic fatigue has proved to cause serious problems.

Mead [2] was one of the first investigators to analyze the dynamic behaviour of such structures by using an approach which combined the hierarchical FEM with the 2D periodic structure theory, to yield a stiffness/mass matrix-eigenvalue problem. Dozio [3] et al presented an analytical-numerical method for rapid prediction of the modal characteristics of rectangular plates and the method demonstrates good agreement with published results and standard finite element analysis. The most commonly used prediction methods and guidelines for choosing an appropriate modelling method for stiffened plates are described in the ESDU [4].

The study into how an acoustic field produces the subsequent structural response is of importance in determining the displacement, stress and fatigue life of stiffened structures. The Joint Acceptance function interpretes how the effective modal forcing is dependent upon the spatial matching of the acoustic excitation and the mode shape [5]. Bozich [6] investigated the response characteristics of beams and flat rectangular panels excited by acoustic field by looking at the double area integral of the mode shape and the cross spectral density of pressure in the Joint Acceptance function introduced by Powell [7], who originally developed the normal mode formulation for the linear response in 1958. Blevins [8]



developed an approximation by assuming the spatial pressure distribution is the same to the mode shape function as a conservative estimation of the subsequent response when the acoustic wavelength is much longer than the structure dimensions.

The purpose of this paper is to predict the acoustic response of stiffened plates by using a semi-analytical model, which is efficient to perform a parametric study concerning the influence of the stiffeners and the modal contribution of dominant modes. An incident harmonic plane wave is assumed due to its fundamental nature. The response to a random sound field is not sought in this paper. Small deflections are also assumed for the plates to confine the response to be linear in what follows, since in most applications the acoustic pressure even at high SPL is usually not large enough to produce a nonlinear deflection.

The remainder of the paper is organized as follows. In section 2, the stiffened plate is modelled analytically by the normal mode method. The resulting mode shape and natural frequencies obtained numerically are combined with the acoustic pressure to calculate the acoustic response from the equation of forced vibration motion. In section 3, the subsequent numerical results for the stiffened plate with different layouts are presented and compared to an unstiffened plate. In section 4, the effect of stiffeners, plate surface area and incident angle are quantified by a set of simulations. The contributions of different modes to the response due to the acoustic field are analysed based on the Joint Acceptance function. Conclusions are then provided, which indicate that the acoustic response of stiffened plates is significantly influenced by the stiffener properties rather than the acoustic field.

## 2. Modelling and solution

The thin plates with small deflection are assumed [9], so the effects of shear deformation and rotary inertia are neglected. The stiffeners attached to the plates are modelled as Euler-Bernoulli beams including the restrained warping effect. The structural modelling outlined in this section are based on the assumed-modes method [10], as applied to the free vibration analysis of ribbed plates by Dozio and Ricciardi. The latter is extended also to high frequency, rendering the acoustic response prediction and subsequent parametric study.

### 2.1. Structural modelling

In Figure 1, the rectangular plate is assumed to be isotropic and linear elastic with a uniform thickness, and is ribbed orthogonally by a set of  $i = 1, 2, \dots, I$  prismatic beams parallel to the  $y$ -axis and a set of  $j = 1, 2, \dots, J$  prismatic beams parallel to the  $x$ -axis on one side of the surface. As a result of plate bending, the stiffeners are subjected to bending and torsional deformations. Dynamic loads arising at the  $i$ th  $y$ -wise plate-beam intersection are modelled as the distributed torsional line moment  $m^i = m^i(y, t)$  and the transverse line force distribution  $f^i = f^i(y, t)$  respectively. Similarly, the dynamic loads arising at the  $j$ th  $x$ -wise intersection are  $m^j = m^j(x, t)$  and  $f^j = f^j(x, t)$  respectively. The location of the  $i$ th  $y$ -wise beam is  $x_i$  and that of the  $j$ th  $x$ -wise beam is  $y_j$ .

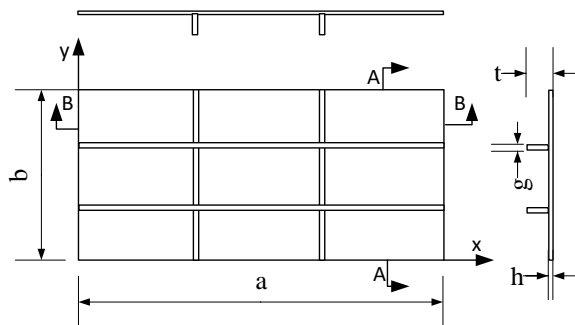


Figure 1. Geometry of a stiffened rectangular plate. Plate dimension,  $a \times b \times h$ ; stiffener cross section dimension:  $g \times t$ ; density  $\rho$ ; elastic modulus,  $E$ ; Poisson's ratio,  $\nu$ ; damping loss factor,  $\eta$ .

Since the force and the moment along the interface act as reactive loads to the plate bending, the equation of motion for the plate is [3]

$$D\nabla^4 w + \rho h \frac{\partial^2 w}{\partial t^2} = - \sum_{i=1}^I (f^i \delta_{x_i} + m^i \delta'_{x_i}) - \sum_{j=1}^J (f^j \delta_{y_j} + m^j \delta'_{y_j}), \quad (1)$$

where  $w(x, y, t)$  is the transverse displacement.  $D = Eh^3/12(1 - \nu^2)$  is the flexural rigidity.  $\nabla^4$  is the biharmonic operator. The force distribution over the surface attached with stiffeners is denoted by the product of the Dirac delta function  $\delta$  and the line force distribution  $f$ . Similarly, the moment distribution is denoted by the product of the unit doublet function  $\delta'$ , i.e. the first derivative of the delta function, and the line moment distribution  $m$ .

The forced bending and torsional motion of the stiffening beams in the  $y$ -wise and in the  $x$ -wise directions are [11]

$$EI^i \frac{\partial^4 w(y, t)}{\partial y^4} + \rho A^i \frac{\partial^2 w(y, t)}{\partial t^2} = f^i, \quad (2)$$

$$EI_w^i \frac{\partial^4 \theta(y, t)}{\partial y^4} - GJ^i \frac{\partial^2 \theta(y, t)}{\partial y^2} + \rho I_0^i \frac{\partial^2 \theta(y, t)}{\partial t^2} = m^i, \quad (3)$$

$$EI^j \frac{\partial^4 w(x, t)}{\partial x^4} + \rho A^j \frac{\partial^2 w(x, t)}{\partial t^2} = f^j, \quad (4)$$

$$EI_w^j \frac{\partial^4 \theta(x, t)}{\partial x^4} - GJ^j \frac{\partial^2 \theta(x, t)}{\partial x^2} + \rho I_0^j \frac{\partial^2 \theta(x, t)}{\partial t^2} = m^j, \quad (5)$$

where  $w(y, t)$  and  $w(x, t)$  are the transverse displacement.  $\theta(y, t)$  and  $\theta(x, t)$  are the angle of twist.  $EI$  is the flexural rigidity.  $\rho A$  is the mass per unit length.  $EI_w$  denotes the warping rigidity associated with the non-uniform warping.  $GJ$  refers to the Saint-Venant torsional rigidity for the uniform torsion and  $\rho I_0$  is the mass moment of inertia per unit length.

Assuming time-harmonic motion, the separable solutions to the bending for the rectangular plate is

$$w(x, y, t) = \sum_{m=1}^M \sum_{n=1}^N \phi_m(x) \psi_n(y) w_{mn} \exp(j\omega t), \quad (6)$$

where the mode shape function is written as the product of two independent beam functions  $\phi_m(x)$  and  $\psi_n(y)$ . The beam functions are determined by the boundary conditions [12], which are assumed initially as simply supported edges in this paper.  $w_{mn}$  is the modal amplitude of the  $(m, n)^{\text{th}}$  mode and  $\omega$  is the circular frequency.

In a similar manner, the separable solutions to the beam bending and torsion are

$$w(y, t) = \sum_{n=1}^N \psi_n(y) w_n \exp(j\omega t), \quad \theta(y, t) = \sum_{n=1}^N \psi_n(y) \theta_n \exp(j\omega t), \quad (7)$$

$$w(x, t) = \sum_{m=1}^M \phi_m(x) w_m \exp(j\omega t), \quad \theta(x, t) = \sum_{m=1}^M \phi_m(x) \theta_m \exp(j\omega t). \quad (8)$$

Substituting the separable solutions equation (6), (7) and (8) into the corresponding equations of motion, the coupled equation of motion for the stiffened plate can be obtained by applying displacement/slope continuity conditions and force/moment equilibriums at the plate-stiffener intersections. It can be expressed in a standard matrix form as

$$(\mathbf{K} - \omega^2 \mathbf{M}) \mathbf{w} = \mathbf{0}, \quad (9)$$

where the mass matrix  $\mathbf{M}$  and the stiffness matrix  $\mathbf{K}$  are real, symmetric and positive definite matrices. The modal amplitudes are grouped into the column vector as

$$\mathbf{w} = [w_{11}, w_{12}, \dots, w_{1N}, w_{21}, \dots, w_{2N}, \dots, w_{mN}, \dots, w_{MN}]^T. \quad (10)$$

The resulting eigenvalue problem, equation (9), can be solved numerically in MATLAB and the lowest  $L$  number of eigenvalue  $\omega_l^2$  and corresponding eigenvectors  $\mathbf{w}_l$  are obtained and retained for the subsequent calculation. The  $l^{\text{th}}$  normal mode of the stiffened plate can be recovered as

$$w_l(x, y) = \mathbf{s}^T \mathbf{w}_l, \quad (11)$$

where

$$\mathbf{s} = [\phi_1 \psi_1, \phi_1 \psi_2, \dots, \phi_1 \psi_N, \phi_2 \psi_1, \dots, \phi_2 \psi_N, \dots, \phi_m \psi_n, \dots, \phi_M \psi_N]^T. \quad (12)$$

The resulting natural frequencies and normal mode shapes will be used as an input for the acoustic response calculation. This method provides quite accurate upper bound solutions for the natural frequency. For example, the average error of the first lowest 60 natural frequencies (up to 300 Hz) is less than 5% for the stiffened plate shown in Figure 1, compared with the FEM results. This is valid

with either simply supported or fully clamped plate edges. The accuracy decreases for a plate with free edges or the free corners for the first several lower mode orders. This is because the first or second mode shape function for these boundary conditions is a linear combination of translation or rotations, rendering zero natural frequency which decrease the accuracy. It converges to a better accuracy again as the mode order increases.

## 2.2. Acoustic response prediction

In Figure 2, an incident plane wave impinges upon the unstiffened surface of the stiffened plate with the particular angles of incidence. For simplicity, the plane wave is assumed to be acting parallel to the plate width direction, i.e. the angle of incidence  $\beta$  along the plate width is zero, unless special statement is made.

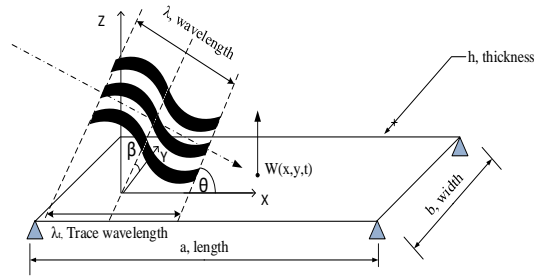


Figure 2. Diagram of an incident harmonic acoustic plane wave. Plate boundary condition, simply supported edges. The plate length lies along the  $x$  direction and the plate width lies along the  $y$  direction.  $\theta$  is the incident angle along the  $x$  direction and  $\beta$  is the incident angle along the  $y$  direction.

The equation of motion for forced vibration of the plate is

$$D\nabla^4 w + \rho h \frac{\partial^2 w}{\partial t^2} = p(x, y, t), \quad (13)$$

where  $p(x, y, t)$  is force distribution, which is the acoustic pressure in this case. The displacement response  $w$  can be represented by finite modes approximation, i.e. adding up the responses of first finite  $L$  number of modes as

$$w(x, y, t) = \sum_{l=1}^L w_l(x, y) q_l(j\omega) \exp(j\omega t), \quad (14)$$

where  $q_l$  is the modal amplitude of the  $l^{\text{th}}$  mode.

Substituting equation (14) into equation (13), the modal amplitude is governed by the relationship

$$q_l(i\omega) = F_0 Z(i\omega) J_l, \quad (15)$$

where the static force  $F_0 = p_0 ab$ , the mechanical impedance  $Z(i\omega) = (\omega_l^2 - \omega^2 + i\eta\omega_l\omega)^{-1}$  and  $J_l$  is the Joint Acceptance function which can be written as

$$J_l(\omega) = (p_0 ab)^{-1} \int_0^a \int_0^b p(x, y, t) w_l(x, y) dx dy. \quad (16)$$

The solutions to equation (16) and then to equation (14), (15) can be numerically found for any mode shape function  $w_l(x, y)$ , which will be presented in next section for the stiffened plate, but in particular the analytical solution is available for the simply supported rectangular plate without stiffeners. For the latter case,

$$J_l(\omega) = \frac{4}{\pi^2 mn} H(\omega) \left(1 - \frac{a^2 \omega^2 \sin^2 \theta}{m^2 c^2 \pi^2}\right)^{-1}, \quad (17)$$

where  $m$  and  $n$  are the numbers of half wavelength along the plate length and width respectively. When  $n$  is odd,  $H(\omega)$  equals to  $\cos((2c)^{-1}a\omega \sin(\theta))$  and  $\sin((2c)^{-1}a\omega \sin(\theta))$  for the odd  $m$  and for the even  $m$  respectively. When  $n$  is even,  $H(\omega) = 0$ , i.e. these modes are not excited. This is because the pressure is cancelled out in a complete wavelength along the plate width where the pressure distribution is uniform in this particular excitation case.

It can be seen from equations (14) – (17) that two factors, the mechanical impedance and the Joint Acceptance, contribute to the modal response. The former gives the inherent FRF for each mode, independent of the acoustic field, and the latter introduces the acoustic-structural coupling due to the

angle of incidence and the mode. Then the total acoustic response can be obtained by multiplying the two factors for each mode and adding them up.

### 3. Numerical results and analysis

Using the equations derived in the paper, numerical results are obtained for simply supported plates with different structural arrangements. Table 1 lists the variables of structural dimensions, material properties and excitation level.

Table 1. Properties and variables for the structure and excitation.

Variable	Symbol	Value	Variable	Symbol	Value
Plate Length (m)	$a$	2.4	Dimension resolution (m)	$dx$	$8 \times 10^{-3}$
Plate Width (m)	$b$	0.9	Dimension resolution (m)	$dy$	$3 \times 10^{-3}$
Plate Thickness (m)	$h$	0.002	Stiffener height (m)	$t$	$3 \times 10^{-2}$
Density (kg/m <sup>3</sup> )	$\rho$	$2.7 \times 10^3$	Stiffener thickness (m)	$g$	$5 \times 10^{-3}$
Elastic modulus	$E$	$71 \times 10^9$	Reference point position	$a_0$	(1.06, 0.38)
Poisson's ratio	$\nu$	0.3	Pressure amplitude (dB)	$p_0$	100dB
Damping loss factor	$\eta$	0.01	Incident angle (rad)	$\theta$	$\pi/4$
			Incident angle (rad)	$\beta$	0

#### 3.1. Natural frequency

In Figure 3(a), four types of plates from cases 1 to 4 are used to make a comparison for different stiffener arrangements. Figure 3(b) shows the natural frequencies of the lowest 20 modes orders for each case.

The natural frequencies of each mode increase from cases 1 to 4. For stiffened plates the natural frequencies tend to occur close together over a small range of values of frequency, which is known as the grouped behaviour. This is because the stiffened plate acts more like a periodic structure. For example, in case 3 the natural frequencies of the lowest 4 modes are near 30 Hz and that of another higher 4 modes are grouped from 40 Hz to 50 Hz. This behaviour becomes more apparent in case 4 for a group of frequencies from 3<sup>rd</sup> mode to 9<sup>th</sup> mode, which are all in the range between 70 Hz and 82 Hz.

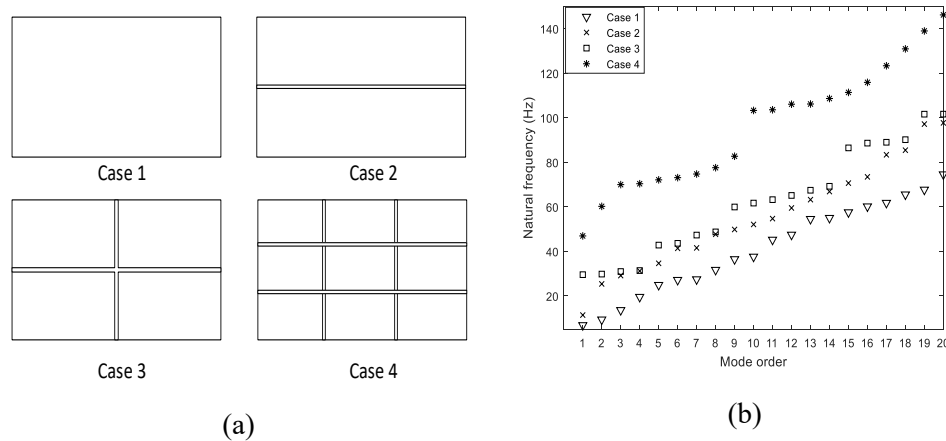


Figure 3. Four types of plates (a) and corresponding natural frequencies (b). Case 1, unstiffened plate; case 2, stiffened plate with 1  $x$ -wise beam; case 3, stiffened plate with 1  $x$ -wise beam and 1  $y$ -wise beam; case 4, stiffened plate with 2  $x$ -wise beams and 2  $y$ -wise beams.

#### 3.2. Acoustic response

Figure 4 shows the displacement FRFs of an arbitrary point  $a_0$ , the position of which is chosen arbitrarily, given in Table 1 previously, so that the point is not on the nodal lines of the lowest modes. For each case, the total response and the modal amplitude are plotted in the bold and thin lines

respectively. A relative high frequency range (up to 1 kHz) is used in the calculation to cover the first 321 natural frequencies for the plates.

The result shows that the response is dominated by the fundamental mode throughout the four cases. The resonance peaks of the stiffened plates move to higher frequencies and tend to be closer compared with those of the unstiffened plates. This is because of the grouped behaviour of the natural frequencies mentioned previously. For example, in case 3 the first order mode and the second order mode have no response due to the even number of half wavelengths along the plate width, but a resonance peak still occurs near 30 Hz, because the third order mode, acting as the fundamental mode, can be excited close to this frequency range. The dips at which the infinitely small values occurs in the modal amplitude, due to the pressure cancellation mentioned previously, are not apparent in the total response.

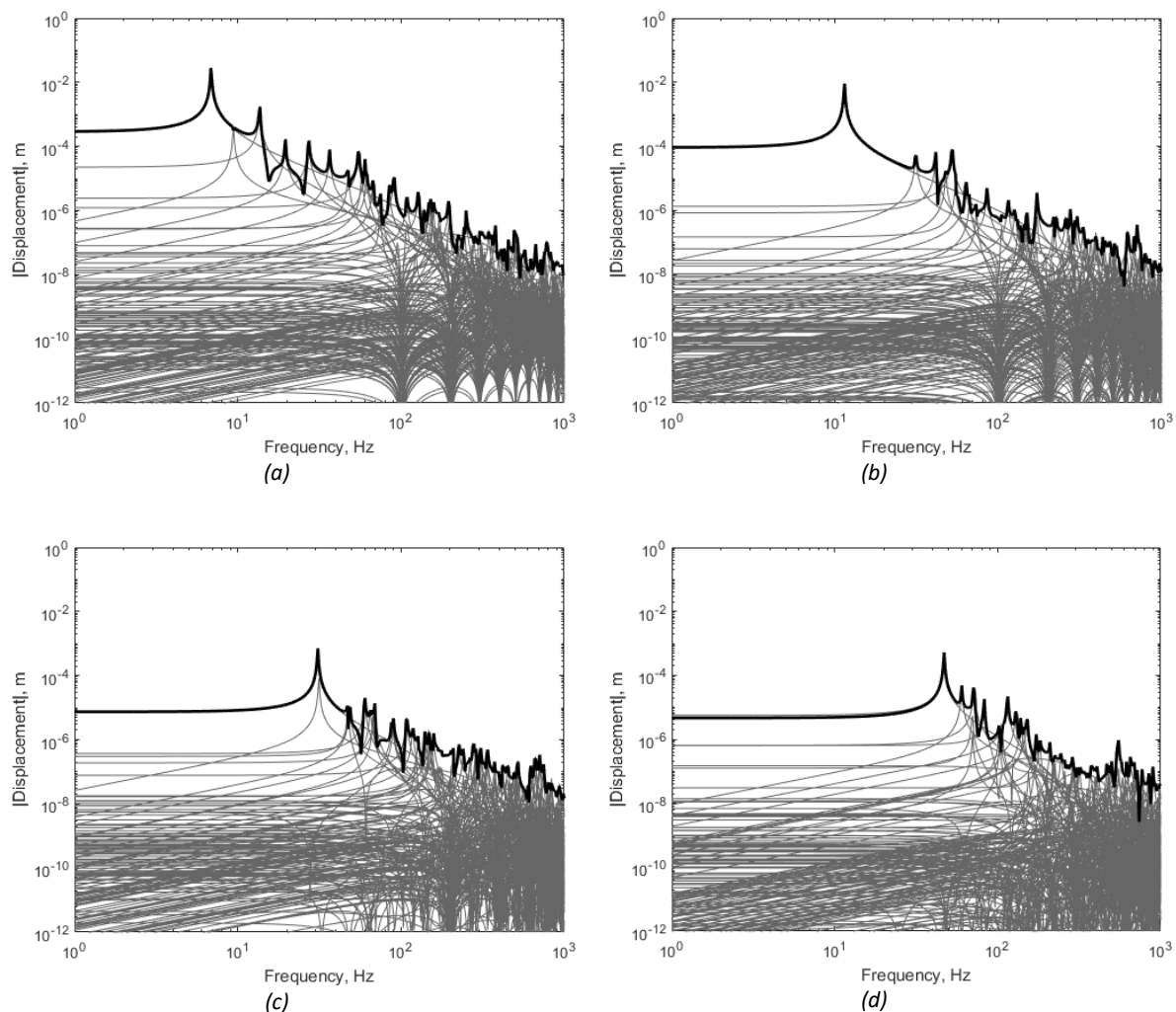


Figure 4. Reference point displacement response for the unstiffened plate, case 1 (a), and stiffened plates, cases 2 to 4 (b) – (d). The thin line is the modal amplitude and the bold line is the total displacement response.

The overall displacement response level is evaluated by the spatial mean square value and by the integral of RMS value versus frequency, shown in Figure 5 (a) and (b) respectively. The result in the latter has been normalized with respect to the overall integral of the total RMS displacement over 1 kHz to highlight the modal contribution to the response of this frequency range.

Figure 5(a) shows that for all cases, the spatial average response is also dominated by the fundamental mode, for which the mean square displacement values are 74 mm<sup>2</sup>, 22 mm<sup>2</sup>, 4 mm<sup>2</sup>, and 2 mm<sup>2</sup>

corresponding to cases 1 to 4, showing a decreasing trend. A similar decreasing trend also occurs for the percentage contribution of the fundamental mode to the total broadband response from cases 1 to 4, which are 83.12%, 80.88%, 78.23% and 58.44% respectively, as shown in Figure 5(b).

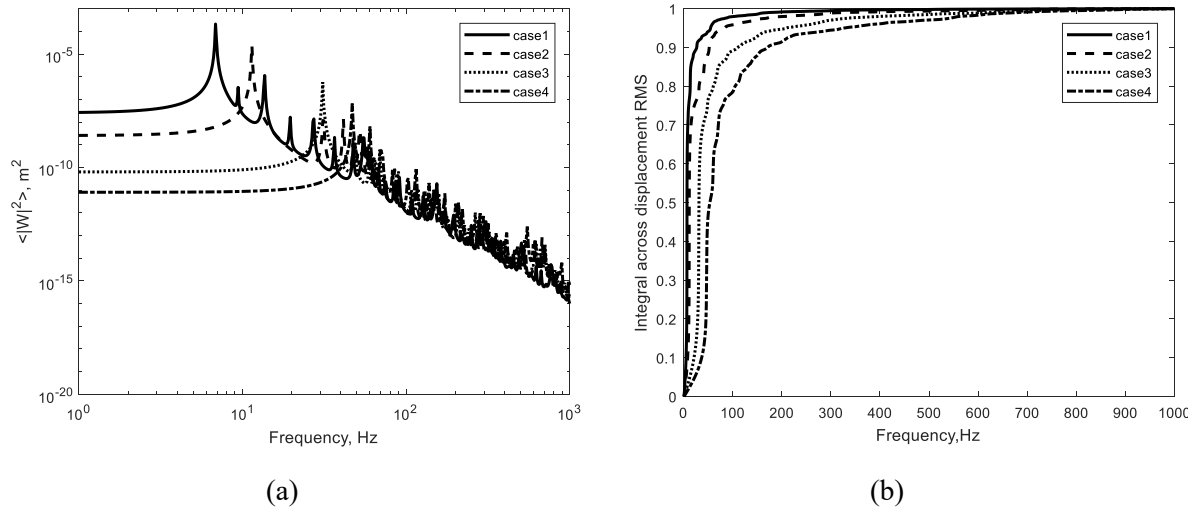


Figure 5. Spatial mean square value of displacement (a) and corresponding normalized integral of the total RMS (b) for each case.

Figure 6 (a) shows the frequency response of the maximum stress points for each case, the position of which are plotted with the small square in Figure 6 (b). The latter also shows the spatial distribution of stress at the frequency rendering the maximum stress.

The maximum stress response has a similar trend to the displacement response. The positions of maximum stress are very different for each case. The highest stress response occurs in the unstiffened plate case 1, located at the plate centre. That for the stiffened plates decreases from case 2 to case 4, located at different areas of the plate due to the influence of the stiffener arrangement.

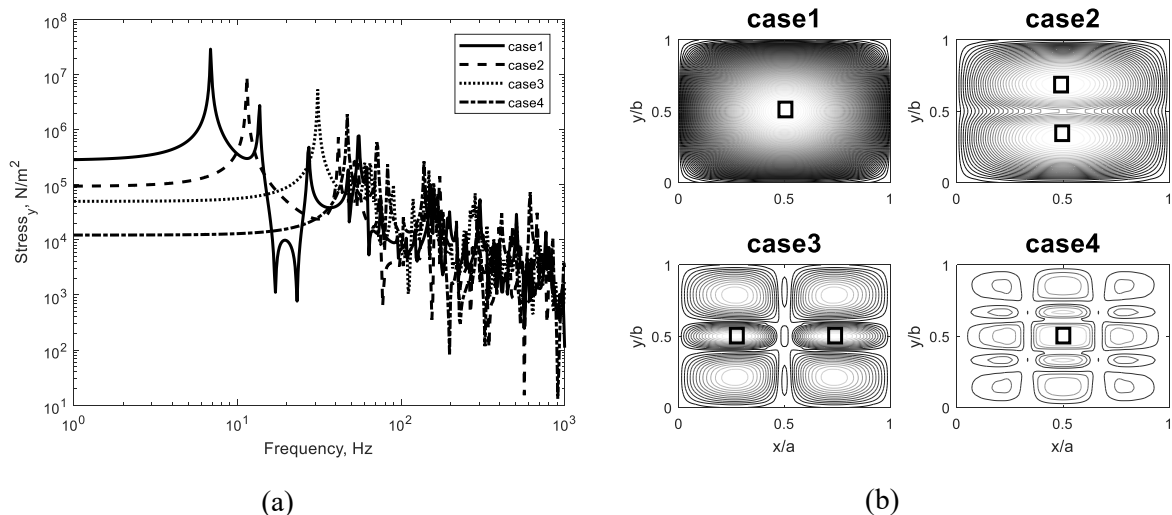


Figure 6. Maximum stress point FRF (a) and distribution when maximum stress occurs (b) for each case

#### 4. Discussion



#### 4.1. Stiffener effect

In the following, the effect of stiffener effect is examined by looking at the local response and the stiffener cross section geometry. Based on the previous results, it is suitable to only consider the fundamental mode response to simplify the analysis.

##### 4.1.1. The response of the local area

In Figure 7, the displacement and stress responses of the stiffened plate corresponding to case 4 are calculated and compared with that of a substructure, which is chosen to be the local bay taken from the centre of the larger plate. Both the larger stiffened plate and the substructure are simply supported around their external edges and are excited by the same acoustic field. The substructure area is one-ninth of the full plate.

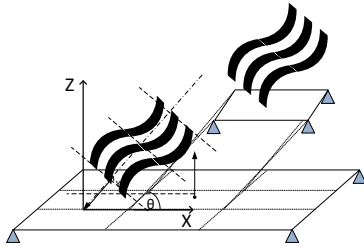


Figure 7. Diagram of two plates with an area ratio of nine.

For reference, the calculation is taken for the unstiffened plate in case 1. This corresponds to comparing two unstiffened plates with different areas. Displacement and the stress responses of the central points are calculated for the fundamental mode in the two cases, and the results are shown in Figures 8.

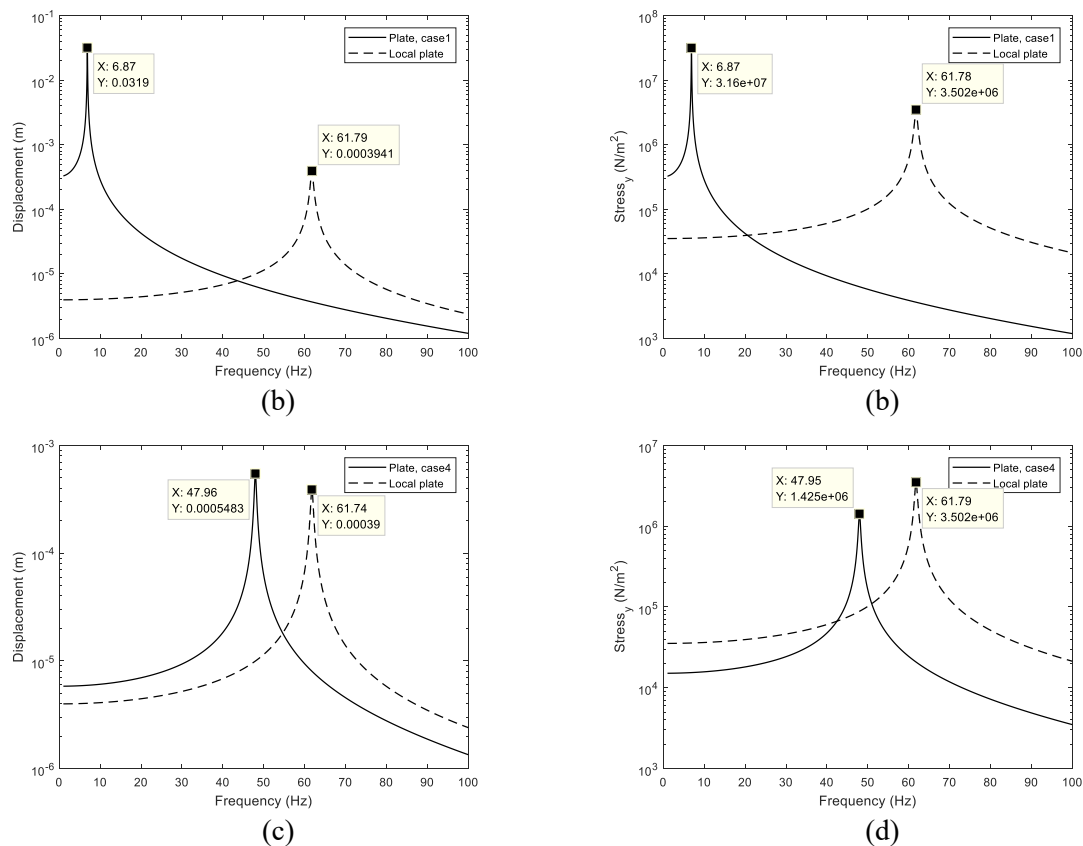


Figure 8. Acoustic response comparison between the larger plate and the local panel bay. Unstiffened plates (a) Displacement, case 1; (b) stress, case 1; Stiffened plate (c) displacement, case 4; (d) stress, case 4. The local plate is the small panel simply supported.

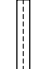
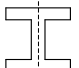
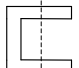
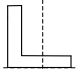
For the unstiffened plate in case 1, the peak displacement response ratio between the plate and the local plate is close to the square of the surface area ratio, and the stress ratio is close to the surface area ratio. This relationship comes from the mechanical impedance expression. The Joint Acceptance functions for the two structures are nearly the same. This is because the acoustic wavelength is large enough when compared with the panel dimension and a uniform pressure field can be assumed.

For the stiffened plate case 4, however, both the displacement response ratio and the stress response ratio between the plate and local bay are much closer to unity compared with the unstiffened case 1. The natural frequencies of these two structures are also closer. This is because the central bay of the plate is stiffened by the constraints of the stiffeners around its edges. The latter acts like the substructure boundary condition which is similar to simply-supported edges.

#### 4.1.2. Cross section geometry

To evaluate the effect of the cross section geometry, the results for three other types of stiffener beam cross sections, I section, C section and L section, are compared with the rectangular beam section. The properties for different cross sections are given in Table 2. The lowest 9 natural frequencies for each cross section in case 4 are calculated and compared with that of the unstiffened plate in Figure 9.

Table 2. Properties for different geometry of the stiffener cross sections. The horizontal dotted line lies on the surface of plate.

Cross section	$EI$ ( $\text{N} \cdot \text{m}^2$ )	$\rho A$ ( $\text{kg/m}$ )	$EI_w$ ( $\text{N} \cdot \text{m}^4$ )	$GJ$ ( $\text{N} \cdot \text{m}^2$ )	$\rho I_0$ ( $\text{kg} \cdot \text{m}$ )
	$3.53 \times 10^3$	0.41	0	30.55	$1.35 \times 10^{-4}$
	$1.09 \times 10^4$	1.08	0.25	96.71	$4.75 \times 10^{-4}$
	$1.09 \times 10^4$	1.08	0.34	96.71	$5.17 \times 10^{-4}$
	$3.65 \times 10^3$	0.74	0	59.46	$2.23 \times 10^{-4}$

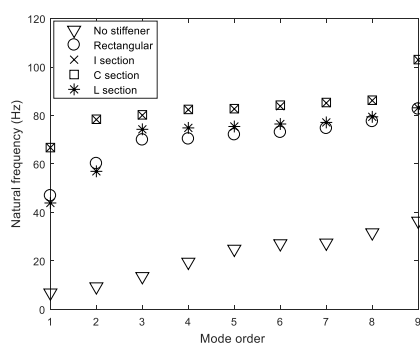


Figure 9. Natural frequencies for different stiffener cross section geometry for case 4 (2  $x$ -wise beams and 2  $y$ -wise beams).

The result shows that the I and C section stiffeners stiffen the plate to a similar extent, which is greater than the L section and the rectangular section. For the fundamental frequency, the response peaks in Figure 9 shift depending on the different cross sections. Due to the influence to the mechanical impedance, the subsequent peaks values in the acoustic response will also be changed.

#### 4.2. The Joint Acceptance and the modal contributions

Equation (15) shows that the acoustic response of stiffened plate is also influenced by the structural-acoustic coupling characterized by the Joint Acceptance function, which is a ratio between the equivalent modal force and a static force represented by a uniform static pressure acting normal to the

plate surface. Figure 10 shows the Joint Acceptance of the five lowest mode orders for each case. The  $x$  axis on the figure is the ratio between the plate free bending structure wavelength and the acoustic trace wavelength. Since the free bending wavelength is the same for the plates, independent of the mode orders, the result only denotes the frequency dependency on the modal force due to the change in the spatial distribution of the acoustic excitation. Here a more generic result is obtained by setting both angles of incidence to  $\pi/4$  to avoid the constant zero value of Joint Acceptance due to the even number of half wavelengths along the plate width or length direction.

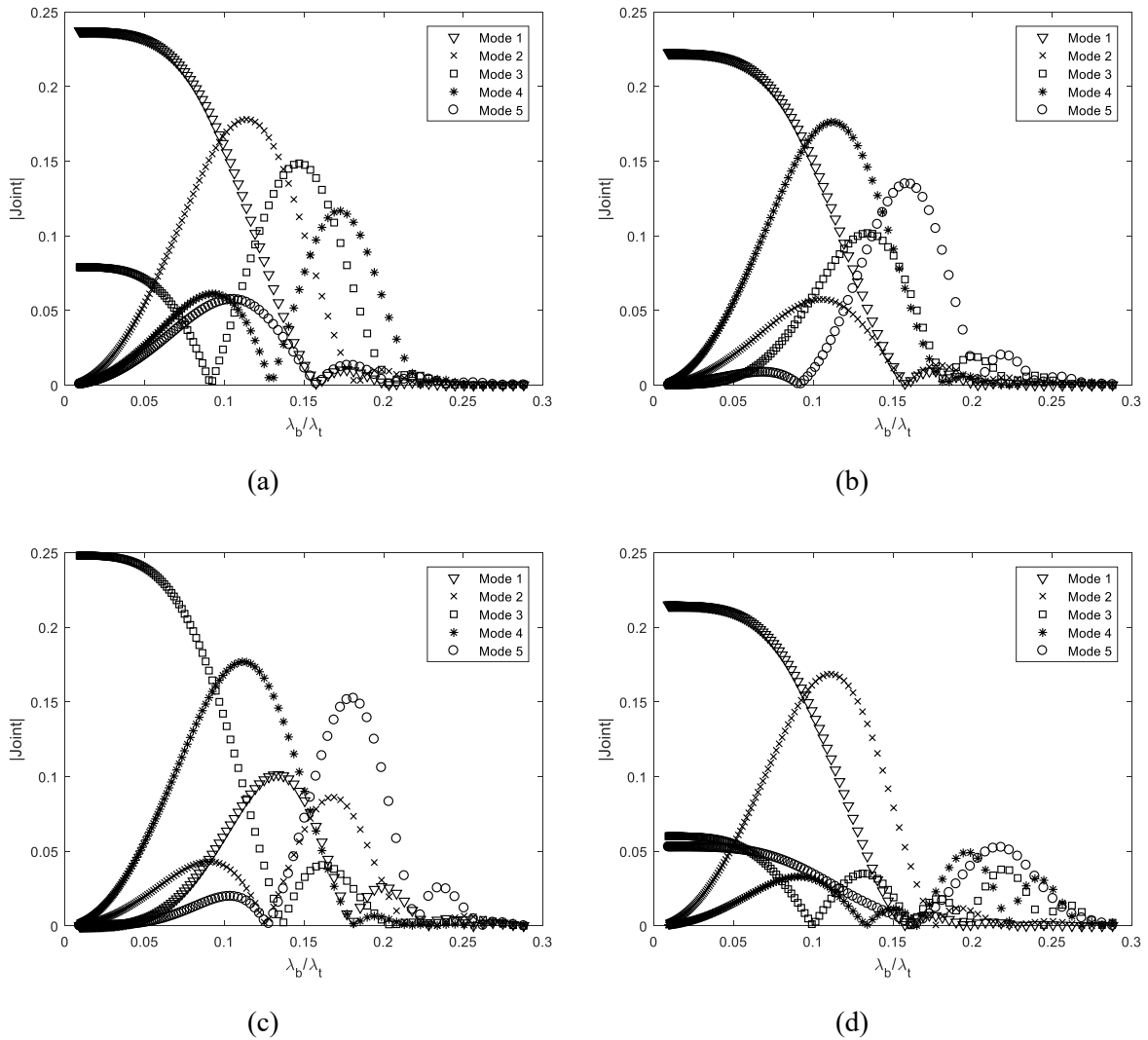


Figure 10. Joint Acceptance function for the five lowest mode orders for each case. (a) – (d) corresponding to cases 1 – 4 respectively.

The result shows the modal contribution due to the structural-acoustic coupling effect. The differences in the Joint Acceptance of the lowest modes for stiffened plates from case 1 to 4 are very small, although these modes correspond to different mode orders. The peak values in the Joint Acceptance in each mode occur when the acoustic trace wavelength matches the structure wavelength.

#### 4.3. Incident angle effect

The angle of incidence contributes to the acoustic response by influencing the structural-acoustic coupling. This ends up in the pressure component in the Joint Acceptance function, independent from

the structural modal characteristics. Hence the effect of the angles can be evaluated by looking at the response of the unstiffened plate to different incident angles.

Figure 11 shows the total displacement response when the incident angle is changed from normal incidence, i.e.,  $\theta = 0$ , to grazing incidence, i.e.,  $\theta = \pi/2$ , for the unstiffened plates excited at its fundamental frequency.

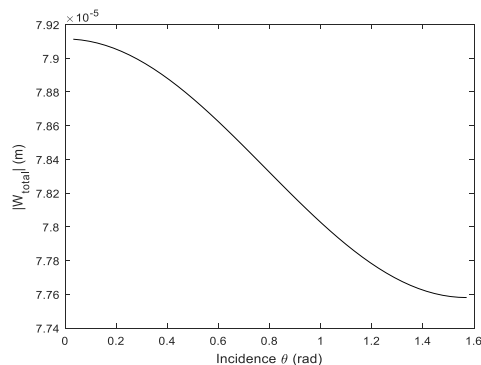


Figure 11. Total displacement response at the fundamental frequency for different incident angles of the acoustic field to the plate surface.

The response becomes smaller as the angle increases. This is due to the influence of the angle on the Joint Acceptance. However, the effect on the total response is very small as the largest change is within a range of 2%. This is because the acoustic wavelength is large compared to the structure dimension, so that the acoustic field can be assumed distributed as uniform pressure amplitude approximately on the plate surface.

## 5. Conclusions

In this paper, the acoustic response of stiffened flat homogeneous plates is evaluated based on a semi-analytical model. The displacement and stress response from the numerical calculation for the plates with different layouts are then given and analyzed. The influences of the stiffeners, surface area, incident angle and modal contribution are discussed. Based on this work, the following concluding remarks for the acoustic response of stiffened plates can be made.

- (1) The modal characteristics of stiffened plates are influenced significantly by the layouts and the cross section geometry of the stiffeners. The grouped behaviour of natural frequencies tends to become apparent for plates with more stiffeners. The I and C section stiffeners add a greater stiffness effect on the plates due to their high flexural, warping and torsional rigidity.
- (2) The acoustic response of stiffened plates is dominated by the fundamental mode, and is influenced by the local constraints added by the stiffener. The maximum response, the spatial mean square response and the percentage contribution of the fundamental mode all decrease when the plate is highly stiffened with an increasing number of stiffeners.
- (3) The mechanical impedance typically contributes much more than the Joint Acceptance and the angle of incidence to the response of the stiffened structures in aerospace applications. The approximations of the Joint Acceptance to simplify the acoustic response prediction is reasonable in engineering practice for complicate stiffened flat plates.
- (4) Following the previous remark, a linear relationship between the maximum stress and the surface area is obtained for the unstiffened plates, based on a response estimation which can be made between plates with the same aspect ratios but different area. It becomes inaccurate, however, for the stiffened plates, because that relationship is changed due to the stiffener local constraints, which are impractical for identification in most applications. Hence, calculations based on predicting the response of a single bay in isolation from the rest of the total stiffened plate is not necessarily accurate.

## 6. References

- [1] Clarkson B L 1994 Review of sonic fatigue technology (Hampton, Virginia: National Aeronautics and Space Administration) pp 5 - 6
- [2] Mead D J, Zhu D C and Bardell N S 1988 Free vibration of an orthogonally stiffened flat plate *J. Sound Vib.* **127** 19-48
- [3] Dozio L and Ricciardi M 2009 Free vibration analysis of ribbed plates by a combined analytical–numerical method *J. Sound Vib.* **319** 681-97
- [4] ESDU 1997 Vibration and Acoustic Fatigue In: *Engineering Sciences Data Unit Design Guide Series*, (London: ESDU International)
- [5] Richards E J and Mead D J 1968 *Noise and acoustic fatigue in aeronautics* (London: Wiley) pp 296-7
- [6] Bozich D J 1962 Spatial Correlation in Acoustic-Structural Coupling *J. Acoust. Soc. Am.* **34** 1989-
- [7] Powell A 1958 On the fatigue failure of structures due to vibrations excited by random pressure fields *J. Acoust. Soc. Am.* **30** 1130-5
- [8] Blevins R D 1989 An approximate method for sonic fatigue analysis of plates and shells *J. Sound Vib.* **129** 51-71
- [9] Timoshenko S and Woinowsky-Krieger S 1959 *Theory of plates and shells* (New York: McGraw-Hill) pp 1-3
- [10] Meirovitch L 1967 *Analytical methods in vibrations* (New York: Macmillan) pp 233-5
- [11] Rao S S 2007 *Vibration of Continuous Systems* (Hoboken: Wiley) pp 344-57
- [12] Leissa A W 1969 *Vibration of Plates* (Columbus, Ohio: Scientific and Technical Information Division, National Aeronautics and Space Administration) pp 41-2

## Acknowledgments

The authors would like to acknowledge the BISE-FEE Joint Laboratory, who funded the project of acoustic fatigue prediction for advanced aerospace structures, and Dozio L., who made available the MATLAB codes used in the paper.